Catalysis Letters Vol. 104, Nos. 1–2, October 2005 (© 2005)
DOI: 10.1007/s10562-005-7432-3

Pd/Pt on Ti-containing mixed oxides as dearomatization catalysts: physico-chemical characterization and activity

Simone Albertazzi[a], Christian Barbieri[a], Antonia Infantes-Molina[b], Antonio Jiménez-López[b], Ramón Moreno-Tost[b], Enrique Rodríguez-Castellón[b], and Angelo Vaccari[a,*]

[a]*Dipartimento di Chimica Industriale e dei Materiali, Alma Mater Studiorum-Università di Bologna, INSTM-UdR Bologna, Viale del Risorgimento, 4, 40136, Bologna, Italy*

[b]*Departamento de Química Inorgánica, Cristalografía y Mineralogía, Facultad de Ciencias, Universidad de Málaga, 29071 Málaga, Spain*

Received 12 June 2005; accepted 24 June 2005

Pd/Pt supported on pure and doped TiO_2 (TiO_2–WO_3 and TiO_2–WO_3–SiO_2) were prepared and characterized by different techniques (XPS, TEM, XRD, H_2-TPR and TPD of ammonia). These catalysts were investigated in the hydrogenation of tetralin at 6.0 MPa, checking also their thio-tolerance by feeding increasing amounts of dibenzothiophene (DBT, 300 and 1000 wt ppm). The catalytic activity followed the order: Pd/Pt–TiO_2 > Pd/Pt–TiO_2–WO_3–SiO_2 > Pd/Pt–TiO_2–WO_3, evidencing a negative role of a second oxide inside TiO_2. The Pd/Pt–TiO_2 catalyst showed high activity regardless of reaction conditions (temperature, contact time, H_2/tetralin ratio) together with a good thio-tolerance up to 300 wt ppm of DBT.

KEY WORDS: Pd/Pt; TiO_2; TiO_2–WO_3; TiO_2–WO_3–SiO_2; decahydronaphthalene or decalin; 1,2,3,4-tetrahydronaphthalene or tetralin; hydrogenation; hydrogenolysid/ring-opening; dearomatization; dibenzothiophene.

1. Introduction

A typical straight run (SR) diesel might contain 20–25% aromatics by volume, while a diesel blended from catalytically cracked stocks (light cycle oil, LCO) could have 40–50% aromatics [1,2]. Since aromatic hydrocarbons have low cetane number, diesel fuels containing a high fraction of aromatics tend to have poor self-ignition qualities. Typical cetane values for straight run diesel are in the range of 50–55; those for highly aromatic diesel fuels are 40–45 or even lower. This gives rise to difficulties in cold starting, increased combustion noise, unburned hydrocarbons (HC) and NO_x due to the increased ignition delay. Increased aromatic contents are also related to higher particulate emissions, due to the fact that high aromatic fuels have a high tendency to deposit on fuel injectors and on other critical components. Such deposits can interfere with proper fuel/air mixing, thus greatly increasing particulate matter (PM) and HC emissions

Some of the polycyclic aromatic hydrocarbons (PAH) are mutagenic and, in some cases, cause cancer in animals after skin painting experiments. As a consequence, stringent fuel specifications (Euro I–V) for gasoline and diesel fractions resulted. In the case of diesel fuels the aromatic level is expected to be lowered to 1 wt% by the end of this decade (Euro V). Traditionally, LCO has been primarily used as low value heating oils. Only a small proportion has been blended into diesel at the expense of lower ignition quality of the diesel pool. Nowadays, this practice is becoming more and more difficult as a result of both these increasing stringent fuel regulations and the increasing demand for diesel car fuels. Production of high quality diesel oils from LCO could not only meet current and future fuel specifications, but also bring potential economic benefits worth billion of dollars.

The development of new catalysts to achieve the targeted aromatic and sulphur levels under mild operative conditions is a key to the objective. Mo, W, Co, Ni or noble metals supported on a wide number of materials have been investigated in hydrogenation of polyaromatics (HYD) and hydrodesulphurization (HDS) reactions [3,4]. Systems supported on TiO_2 exhibited higher activities than catalysts supported on γ-Al_2O_3 [5,6]. However, thermal instability, low surface area and poor mechanical properties are significant drawbacks. In order to overcome these disadvantages, different methods of mixing TiO_2 with other oxides, such as Al_2O_3, SiO_2 and ZrO_2, have been studied by several authors [7–11]. The catalytic results in HYD and HDS reactions suggested that an increase in dispersion may be responsible for an increase in activity [3].

In recent years, noble metals have been widely investigated [12–14] as active phases for hydrotreating catalysts, since only a two-stage hydrotreating process, using noble metals catalyst in the second stage, can achieve deep levels of aromatic hydrogenation under mild operating conditions (i.e., moderate H_2 pressure and low temperature). Since noble metal catalysts are

* To whom correspondence should be addressed.
E-mail: vacange@ms.fci.unibo.it

1011-372X/05/1000–0029/0

easily poisoned by small amounts of S-containing compounds, the HDS catalyst in the first-stage reactor has to reduce the S-level up to a few wt ppm. Enhanced activity and thio-tolerance have been claimed for the Pd/Pt couple on several supports [15,16].

Aim of this study was to combine these two important aspects (support and active phase) to design new HYD catalysts. Pd/Pt supported on commercial TiO_2, TiO_2–WO_3 and TiO_2–WO_3–SiO_2 were prepared, characterized by using a battery of techniques (XPS, TEM, XRD, H_2-TPR and TPD of ammonia), and investigated in the hydrogenation of tetralin (1,2,3,4-tetrahydronaphthalene, THN) at 6.0 MPa, chosen as a model reaction for the HYD of LCO feeds. The reaction is rather complicated, since side reactions also occur (figure 1). Tetralin can be hydrogenated to the saturated (cis + trans) decalin (decahydronaphthalene or DeHN). On the other hand, cracking reactions to low molecular weight compounds (LMW compounds, having six or fewer atoms of C) occur and are not wished for, being outside the diesel range. Finally, unwanted dehydrogenation to naphthalene (NPH) and polycondensation reactions to tar also occur. Useful compounds are those derived from hydrogenolysis/ring-opening reactions, called high molecular weight compounds (HMW, mainly alkylcyclohexanes, alkylbenzenes, methylindanes and methylindenes, spyrodecane), having high cetane numbers [17].

2. Experimental

2.1. Catalyst preparation and characterization

The commercial TiO_2, TiO_2:WO_3 (91:9 wt%) and TiO_2:WO_3:SiO_2 (81:9:10 wt%) supports were supplied by Millenium Chemicals. One weight percent of Pd/Pt [atomic ratio (a.r.) = 4.0], already evidenced as the best active phase [17,18], was supported by incipient wetness technique using an aqueous solution of H_2PtCl_6 and $Pd(NO_3)_2$ (Pressure Chemicals, analytical grade). After the drying, the samples were calcined at 500 °C for 5 h to obtain the final catalysts (table 1).

BET surface area, pore volume and distribution were calculated from N_2 adsorption at −196 °C carried out with a Micromeritics ASAP 2020 glass volumetric apparatus, previously outgassing the samples at 200 °C and 10^{-4} mbar overnight. Transmission electron micrographs (TEM) were obtained by using a Philips CM 200 Supertwin-DX4 microscope. Samples were dispersed in ethanol and a drop of the suspension was put on a Cu grid (300 mesh). Powder X-ray diffraction (XRPD) patterns were obtained by using a Siemens D5000 diffractometer, equipped with a graphite monochromator and using CuKα radiation ($\lambda = 0.15418$ nm, 35 mA, 35 mV), recording the patterns in the $2\theta = 10.0$–80.0 ° range.

X-ray photoelectron (XPS) spectra were collected using a Physical Electronics PHI 5700 spectrometer with non-monochromatic AlKα and MgKα radiations (1486.6 and 1253.6 eV, respectively; 300 W, 15 kV) and with a multi-channel detector. Spectra of powder samples were recorded in the constant pass energy mode at 29.35 eV, using a 720μm diameter analysis area. Charge referencing was measured against adventitious carbon (C 1 s at 284.8 eV). A PHI ACCESS ESCA-V6.0 F software package was used for acquisition and data analysis. A Shirley-type background was subtracted from the signals. Recorded spectra were fitted using Gauss–Lorentz curves in order to determine the binding energy of the different element core levels more accurately.

Temperature-programmed desorption of ammonia (NH_3-TPD) was used to determine the total acidity of the

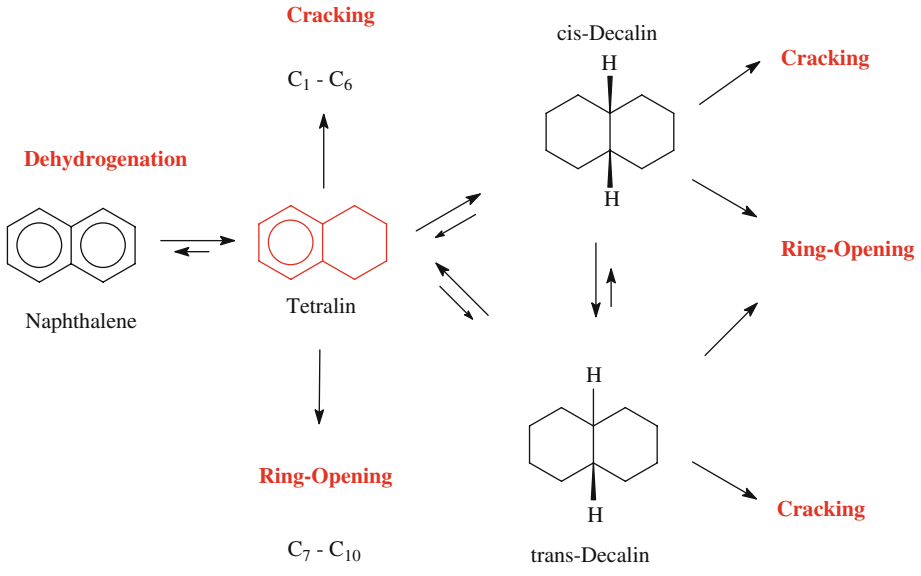

Figure 1. Proposed reaction pathway for the hydrogenation of THN.

Table 1
Composition of the supports and catalysts

Sample	Support	Active phase
CAT51	DT51–TiO_2	1 wt.% Pd/Pt = 4.0 a.r.
CAT52	DT52–TiO_2:WO_3 = 91:9 wt.%	1 wt.% Pd/Pt = 4.0 a.r.
CAT58	DT58–TiO_2:WO_3:SiO_2 = 81:9:10 wt.%	1 wt.% Pd/Pt = 4.0 a.r.

supports. Before the adsorption of ammonia at 100 °C, the samples were treated at 450 °C in a 50 mL/min He flow for 60 min. After evacuation under vacuum of the physically adsorbed NH_3, the TPD tests were performed between 100 and 500 °C, with a heating rate of 10 °C/min. The evolved ammonia was analyzed by an on-line gas chromatograph (Shimadzu GC-14A) equipped with HWD.

H_2 temperature-programmed-reduction (H_2-TPR) experiments were carried out on the catalysts previously calcined at 500 °C for 5 h. The H_2 consumption was studied between 100 and 550 °C, using a 48 mL/min flow of Ar/H_2 (10 vol% of H_2) and a heating rate of 10 °C/min. H_2O produced in the reduction reaction was eliminated by passing the gas flow through a cold finger (−80 °C). The H_2 consumption was determined by an on-line gas chromatograph (Shimadzu GC-14A) provided with HWD. Metal dispersion, metal surface area and the sizes of metal crystallites were evaluated from H_2 chemisorption at 25 °C by using a Micromeritics ASAP 2010C apparatus, after a cleaning step of the samples carried out under He flow at 400 °C and a further reduction step with H_2 flow at 500 °C. The noble metals were supposed to be fully reduced before the analysis, given the high temperature of the reduction treatment.

2.2. Determination of the catalytic activity

The hydrogenation of tetralin was performed in a high-pressure fixed-bed continuous-flow stainless steel reactor (9.1 mm internal diameter and 230.0 mm length), operating in the down-flow mode. The reaction temperature was measured with a J-type thermocouple placed inside, in direct contact with the top part of the catalytic bed. The organic feed consisted of a solution of tetralin in *n*-heptane (10 wt%), supplied by means of a Gilson 307SC piston pump (model 10SC). A fixed volume of catalyst (3 mL, 0.85–1.00 mm particle size) was used in all the studies. Before the activity tests, the catalysts were reduced *in-situ* at atmospheric pressure with a 60 mL/min flow of H_2 at 400 °C for 1 h, with a heating rate of 15 °C/min. Catalytic activity was measured at 6.0 MPa and different temperatures (from 275 to 375 °C), contact times (τ ranging from 3.6 to 1.8 s), and liquid hourly space velocities (LHSV between 4.0 and 8.0 h^{-1}). The thio-tolerance of the catalysts was checked by adding 300 or 1000 wt ppm of dibenzothiphene (DBT) to the organic feed at 315 °C, checking again the activity after the DBT removal. The H_2/tetralin molar ratios were between 15.0 and 9.0. The reaction was kept in steady state conditions for 1 h and the liquid samples were collected and kept in sealed vials for subsequent analysis, performed using both a Hewlett-Packard 5988A mass spectrometer and a Shimadzu GC-14B gas chromatograph, equipped with FID and a capillary column (TBR-1).

3. Results and discussion

3.1. Chemical-physic characterization

Surface area and pore volume values of the supports (table 2) follow the order: DT58 (TiO_2:WO_3:SiO_2 = 81:9:10 w/w/w) > DT52 (TiO_2:WO_3 = 91:9 w/w) > DT51 (TiO_2), according to the values reported for the single oxides: $SiO_2 > WO_3 > TiO_2$ [19–21]. The surface area and pore volume values of the catalysts before reaction follow the same order, although they are significantly lower than those of the corresponding supports, thus highlighting partial pore occlusion by the metals. Also, the surface area and the pore volume values of the catalysts after reaction follow the same order, but are even lower, evidencing a further surface occlusion attributable to the deposition of tar formed by side reactions.

Table 2
Chemical-physical characterization of the supports and catalysts before and after reaction

Sample	Surface area (m^2/g)	Pore volume (mL/g)	Average pore size (nm)	Acidity (μmolNH_3/gcat)	D (%)	Metal surface area (m^2/gmetal)	Average metal particle size (nm)
DT51	77	0.297	15.47	325	–	–	–
DT52	104	0.345	13.25	485	–	–	–
DT58	126	0.409	13.02	360	–	–	–
CAT51[a]	59	0.195	13.19	–	6.4	24.6	10.4
CAT52[a]	100	0.251	10.00	–	3.1	11.8	21.7
CAT58[a]	106	0.320	12.11	–	2.1	8.0	32.0
CAT51[b]	66	0.248	15.01	–	2.7	10.3	25.1
CAT52[b]	83	0.234	11.25	–	2.2	8.3	30.9
CAT58[b]	92	0.295	12.76	–	2.0	7.7	33.4

[a] Before reaction.
[b] After reaction.

However, the elemental C-analysis carried out on CAT51 before (5.24 wt% of C, due to residual carbonates from the sol–gel synthesis, in agreement with XPS analysis, see below) and after reaction (2.06 wt%) does not support this hypothesis. Thus, this decrease may be due to the increase of metal particle sizes after reaction, as will be commented later.

The N_2 adsorption–desorption isotherms at −196 °C are similar for all the solids and can be classified as type IV isotherms based on the IUPAC classification [22,23], since they feature the hysteresis loop generated by the capillary condensation in mesopores. The N_2 adsorption–desorption isotherms (figure 2a) and the corresponding BJH adsorption plot (figure 2b) are reported for CAT58, as the typical example for all the investigated materials. The average pore sizes of the samples can be allocated in the mesoporous range (2–50 nm) and fit well with the sizes of the cumbersome molecules belonging to a typical LCO feed.

All the noble-metal-containing catalysts show low metal dispersion values (D) (table 2), notwithstanding the relatively high surface area value of the support; furthermore, since the metal dispersion depends on the interaction active phase/support, the presence of WO_3 and/or SiO_2 significantly worsens the already poor properties of TiO_2. After reaction, these values further decreased, probably due to segregation phenomena. It is noteworthy that the metallic particle sizes are higher than the corresponding pore diameters, thus suggesting that metals did not diffuse significantly inside the pores and, consequently, the catalytic processes occur mainly on the external surface.

The low dispersion determined by H_2-chemisorption is confirmed also by the TEM replica (figure 2): CAT51 (figure 3a) shows almost uniform particles < 50 nm, while CAT52 (figure 3b) shows a high number of particles > 50 nm, together with smaller particles. Finally, CAT58 sample shows (figure 3c) smallest metallic particle sizes, aggregated together while forming large agglomerations.

The acidity of the supports determined by NH_3-TPD (table 2) evidences lower values than conventional hydrotreating catalysts [13,24–26]. The acidity drastically increases the rate of tar deposition and/or the yield in light hydrocarbons formed by cracking reactions [13]. Among the supports, the acidity follows the order: DT52 (TiO_2:WO_3 = 91:9 wt:%) > DT58 (TiO_2:WO_3:SiO_2 = 81:9:10 wt.%) > DT51 (TiO_2), according to what was proposed for the single oxides: $WO_3 > TiO_2 > SiO_2$ [27–30]. For all the supports, the NH_3-desorption achieves its top (30–40% of the total acidity) between 200 and 300 °C, thus highlighting mainly medium strength acid sites. These results may be positive to limit unwanted cracking and coking reactions, but have a negative effect on the thio-tolerance and hydrogenolysis/ring-opening activity. As already reported [31], the acidities of noble metal containing catalysts are not significant, since the possible occurrence on these samples of ammonia decomposition to nitrogen, detectable only by mass spectroscopy [32], and of ammonia chemisorption, with not exactly known stoichiometry, on the surface of the reduced noble metals. Finally, in the case of the generation of the active metal sites by reduction of cationic species, the surface acidity depends on the evolution of the metal/support interaction during the reduction [33].

The TPR results (figure 4) evidence that the noble metals are completely reduced at temperatures lower than 400 °C, by confirming that the noble metals were totally reduced before the H_2-chemisorption analysis; thus, the *in situ* reduction before the catalytic tests were carried out at this temperature for all the catalysts. However, the three catalysts show considerably different edges of the reduction peaks, although all had the same Pd/Pt ratio and total amount: CAT58 (≅250 °C), CAT 51 (≅225 °C) and CAT52 (≅185 °C), reflecting different

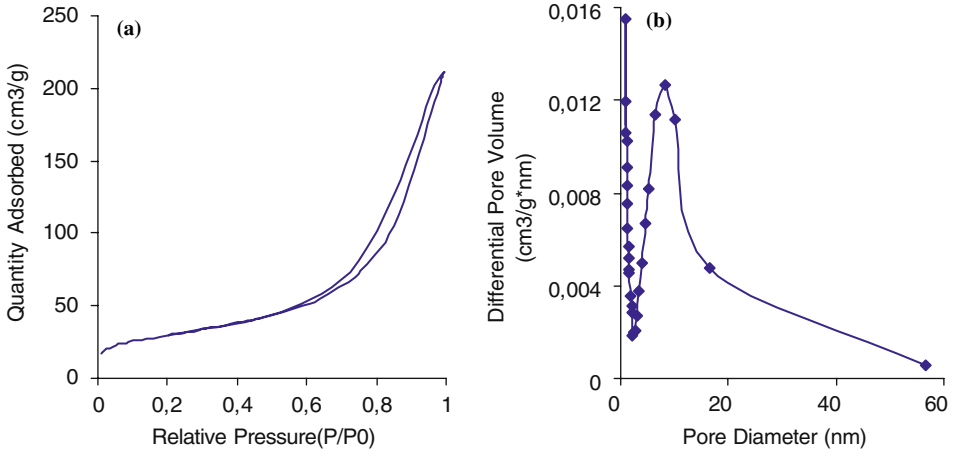

Figure 2. N_2 adsorption–desorption isotherm at −196°C (a) and corresponding pore size distribution (b) for CAT58.

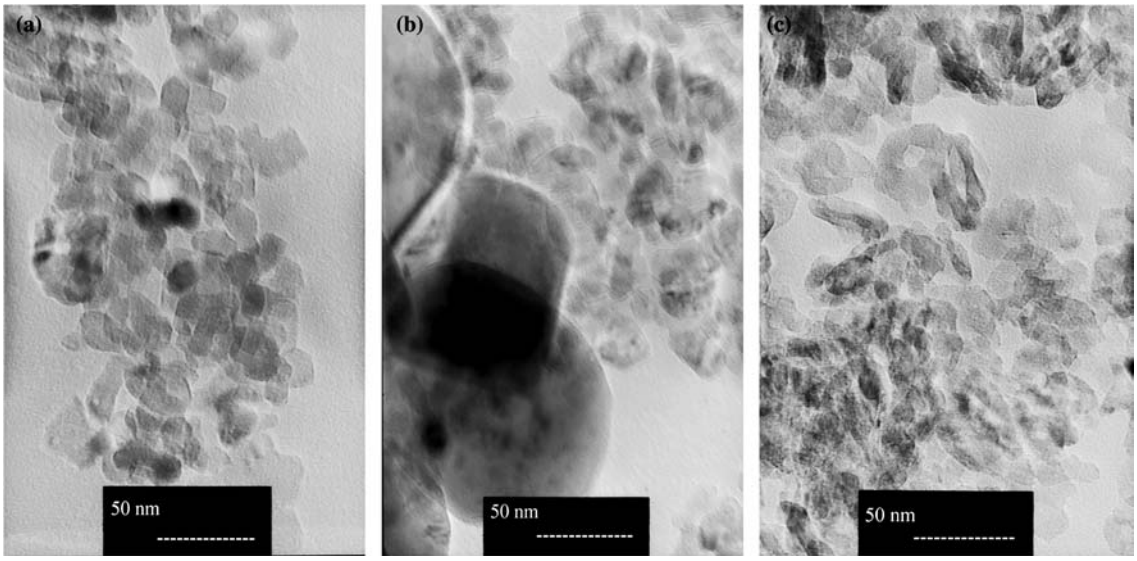

Figure 3. TEM replica of the CAT51 (a), CAT52 (b) and CAT58 (c) samples.

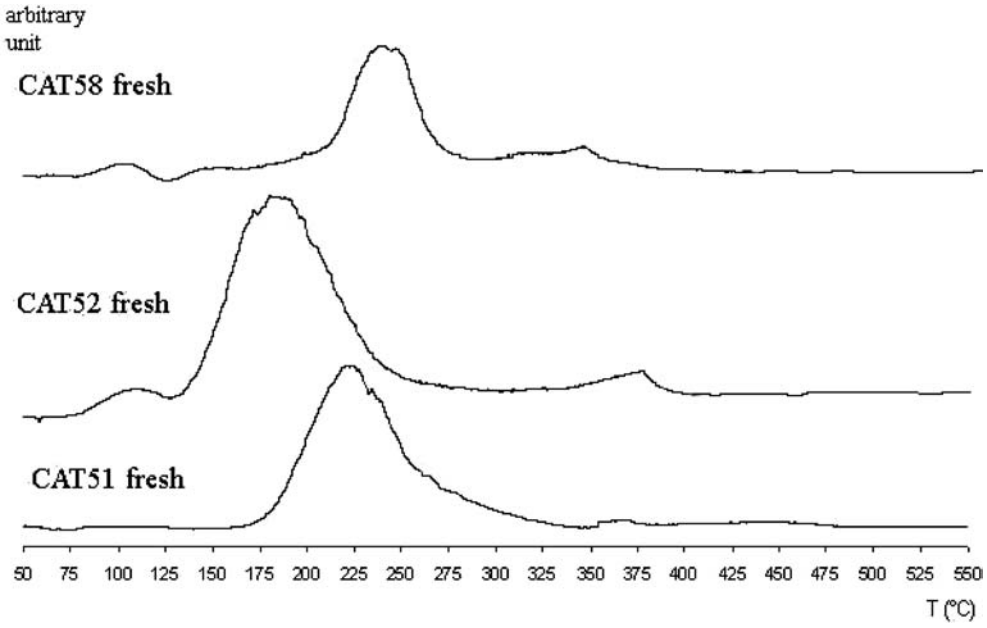

Figure 4. TPR patterns of the catalysts before reaction.

interaction of Pd and Pt with the supports. XRD patterns show for all the solids only the peaks of TiO_2 anatase (figure 5), regardless of the support composition; neither segregated noble-metal oxide nor metal phases were detected either before reduction or after the catalytic tests, thus evidencing a stable metal dispersion in all catalysts.

XPS spectra of all the solids do not show significant differences between the support and the corresponding catalysts, both before and after reaction (figure 6). All the supports show peaks attributable to C (as carbonate), S (as sulphate) and N (as nitrate), coming from the sol–gel synthesis. In the samples containing WO_3, bridges Ti–O–W and W–OH have also been detected, which are mainly responsible for the enhanced acidity. On the contrary, no bridges Ti–O–Si have been detected in the samples based on TiO_2–WO_3–SiO_2, thus suggesting that silica precipitated alone after the formation of the TiO_2–WO_3 co-gel. This process may be relevant in the industrial preparation, since it allows a SiO_2 layer (with high surface area and pore volume) to be obtained on the solid surface, as evidenced by its higher concentration detected on the surface (15.36 atomic% of Si_{2p}). In the catalysts before reaction, the concentration of the noble metals on the surface was lower than the nominal value, thus confirming the bad dispersion obtained in the metal loading, because Pd and Pt in the lower layers of the large agglomerates cannot be detected by XPS.

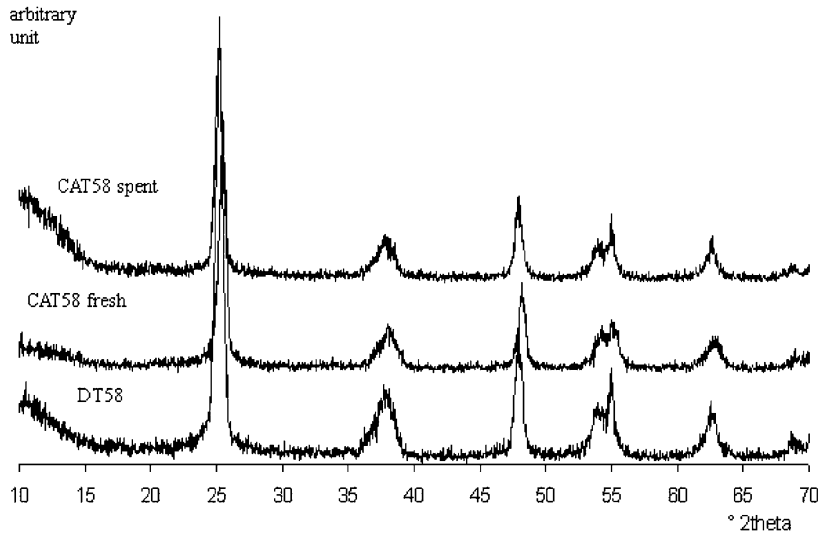

Figure 5. XRPD patterns of the support DT58 and the catalyst CAT58, before and after reaction.

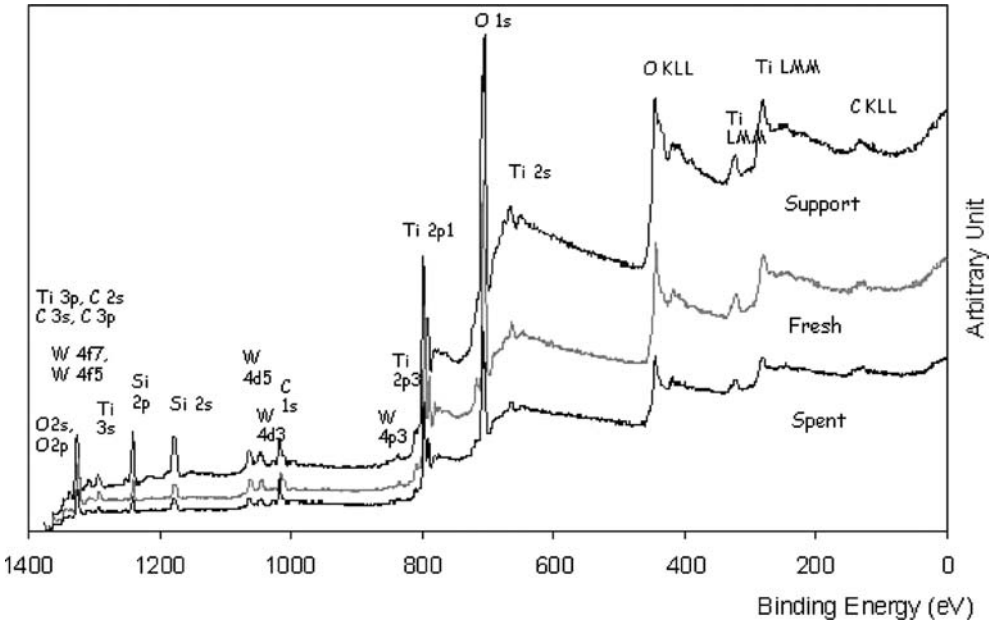

Figure 6. XPS spectra of the support DT58 and the catalyst CAT58, before and after reaction.

The Pd 3d core level spectrum for CAT51 before reaction shows a doublet Pd $3d_{5/2}$ and Pd $3d_{3/2}$ typical of Pd^{2+} (figure 7). The sample supported on TiO_2 shows the highest noble metal concentration ($Pd_{3d} = 0.10$ and $Pt_{4f} = 0.11$, as atomic%), according to its highest dispersion, already evidenced by H_2-chemisorption and TEM. Furthermore, it contains a small amount of Pd^{2+} after reaction (figure 6), unlike the other two spent catalysts, which show only the presence of Pd^0 and Pt^0.

3.2. *Catalytic activity of CAT51 (1.0 wt% of Pd/Pt = 4.0 a.r. on TiO_2)*

CAT51 shows a high hydrogenation activity to (cis + trans) DeHN (table 3), which decreases by increasing the reaction temperature, due to the mild exothermicity of the hydrogenation reaction. Also a considerable amount of naphthalene (4.0%) was detected at the maximum temperature investigated (375 °C). The losses in the C balance increase with temperature, according to the endothermic nature of the cracking reactions, although they always remain low. After the test at 375 °C, the activity at 275 °C was examined again in order to check the thermal stability of the catalyst under reaction conditions. The conversion of THN and the yield in DeHN are higher than the initial values, suggesting a further activation during the tests. The yield in hydrogenolysis/ring-opening HMW compounds remained quite low also increasing the temperature

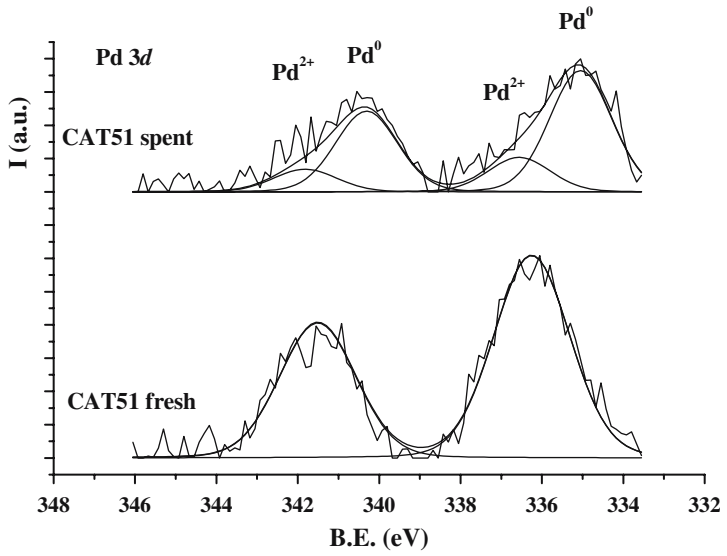

Figure 7. Pt 3d core level spectra for the catalyst CAT51, before and after reaction.

Table 3
Catalytic activity of CAT51 as a function of the reaction conditions

	THN conversion (%)	Yield in DeHN (cis + trans) (%)	Yield in NPH (%)	Yield in HMWs (%)	C-balance losses (%)
Temperature (°C)[a]					
275	84.5	76.0	0.1	1.9	6.5
315	95.3	84.3	0.1	2.2	8.7
350	93.3	80.8	0.5	2.4	9.6
375	79.1	61.0	4.0	3.4	10.7
275	96.1	85.1	0.1	1.9	9.0
Contact time (s)[b]					
3.6	95.3	84.3	0.1	2.2	8.7
2.7	96.4	87.6	0.2	1.7	6.9
1.8	99.9	92.3	0.0	1.3	6.3
H_2/THN (mol/mol)[c]					
15.0	95.3	84.3	0.1	2.2	8.7
12.0	99.5	86.0	0.0	1.0	12.5
9.0	98.3	75.1	0.1	0.9	22.2
DBT (wt. ppm)[d]					
0	97.1	91.4	0.0	1.3	4.4
300 (51 wt. ppm S)	99.9	94.2	0.0	1.4	4.3
1000 (170 wt. ppm S)	39.6	36.7	0.1	1.7	1.1
0	91.7	88.4	0.0	2.2	1.1

W_{cat} = 2.95 g: [a]contact time = 3.6 s, LHSV = 4 h^{-1}, H_2/THN molar ratio = 15.0; [b]Temperature = 315°C, H_2/THN molar ratio = 15.0; [c]Temperature = 300°C, contact time = 3.6 s, LHSV = 4 h^{-1}; [d]Temperature = 315°C, contact time = 3.6 s, LHSV = 4 h^{-1}, H_2/THN molar ratio = 15.0.

(mild endothermic reaction), probably due to the medium-weak acidity of the support. The best performances were observed at 315 °C – although at this temperature the catalyst shows mainly a hydrogenation activity – and this temperature was chosen for the further tests.

On decreasing the contact time, both the conversion of THN and the yield in DeHN increase, while the yield in the consecutive products (formed by hydrogenolysis/ring-opening and cracking reactions) decreases slightly and dehydrogenation to NPH remains negligible. On decreasing the H_2/THN molar ratio, the yield in HMW compounds further decreases, while the losses in the C balance increase by more than 20%, confirming the requirement for a large H_2 excess [12–15,18,34]. Although THN conversion reaches maximum for a molar ratio equal to 12.0, the losses in the C losses increased by decreasing the excess H_2, with minimum value together with the highest yield in DeHN for the H_2/THN = 15.0 molar ratio.

The activity is maintained up to 300 wt ppm of DBT (corresponding to 51 wt ppm of S), a typical amount coming out from a HDS unit placed before the HYD stage. On feeding 1000 wt ppm of DBT, the catalytic performance worsens, although the initial activity was

almost totally recovered by removing the DBT from the feed, thus suggesting an almost reversible poisoning. To this end, elemental S analysis carried out on this sample before (0.108 wt% of S, due to residual sulphates in the synthesis gel, as evidenced by XPS analysis) and after reaction (0.001 wt% of S) confirms that irreversible bo nds between Pd and/or Pt and S were not formed. This indicates that the poisoning is due to a strong but reversible adsorption of the DBT on the metal sites. This catalyst shows better performances in presence of DBT than a previous 2.0 wt% Pd/PT on Zr-doped mesoporous silica, although – due to the lower acidity of the TiO_2 support – the formation of HWM products was smaller [18].

3.3. Activities of CAT52 [1.0 wt% Pd/Pt = 4.0 a.r. on TiO_2:WO_3 (91:9 wt%) and CAT58 1.0 wt% of Pd/Pt = 4.0 a.r. on TiO_2:WO_3:SiO_2 (81:9:10 wt%)] samples

CAT52 sample shows a very low conversion of THN and yield in DeHN at all the investigated temperatures (table 4). At 350 and 375 °C good yields in HMW compounds are obtained, according to the higher support acidity, although the yield in NPH is also significant. The losses in the C balance are moderate regardless of the temperature. When repeating the test at 260 °C, an early deactivation was evident, since worse results were obtained in comparison to the initial test at the same temperature.

CAT58 also shows a low conversion of THN and yield in DeHN. Since the support acidity is relatively high, increased yields in HMW compounds are obtained at 350 and 375 °C, together with high yield values in NPH. The losses in the C balance are below 20% even at the highest temperature (375 °C). Also for this sample, by repeating the test at 275 °C, the catalytic performances worsen, thus highlighting poor stability. The performances of both CAT52 and CAT58 are lower than those observed for CAT51, due to the low metal dispersion determined for these catalysts.

3.4. Comparison of the activities for the three catalysts investigated

Figure 8 show the catalytic performances of the investigated samples at both 275 and 315 °C, normalized for weight unit of catalyst employed. The tetralin conversion (C THN) and the yield in decalin (Y DeHN) decrease according to the following scale: CAT51 > > - CAT58 > CAT52, thus evidencing that the addition of other oxides worsens the performances of TiO_2. On the other hand, no significant differences are noted in both the yield in naphthalene (Y NPH) and the losses in the C balance. Only CAT58 shows interesting yield values in hydrogenolysis/ring-opening compounds (Y HMW), thus evidencing the requirement of a tailored surface acidity to form compounds having high cetane number. This may be obtained by introducing WO_3 in the TiO_2, although this also gives rise to a decrease in catalyst stability in the reaction conditions.

4. Conclusions

1 wt% Pd/Pt (4.0 as atomic ratio) was supported on TiO_2, TiO_2–WO_3 (91:9 wt%) and TiO_2–WO_3–SiO_2 (81:9:10 wt%) were fully characterized and investigated in the hydrogenation of tetralin at 6.0 Mpa in different reaction conditions, while checking also the thio-tolerance by feeding increasing amounts of DBT. The introduction of WO_3 and/or SiO_2 in the synthesis gel increased textural properties, such as surface area and pore volume, as well as the acidity, due to the formation of W–OH bridges at the solid surface. However, the metal dispersion was lower than that of Pd/Pt on TiO_2, as confirmed by H_2-chemisorption, XPS and TEM analyses. This accounts for the order of activity observed in the catalytic tests: Pd/Pt–TiO_2 > Pd/Pt–TiO_2–WO_3

Table 4
Catalytic activities of CAT52 (W_{cat} = 3.16 g) and CAT58 (W_{cat} = 2.59 g) as a function of the reaction temperature (contact time = 3.6 s, LHSV = 4 h^{-1}, H_2/THN molar ratio = 15.0)

Temperature (°C)	THN conversion (%)	Yield in DeHN (cis + trans) (%)	Yield in NPH (%)	Yield in HMWs (%)	C-balance losses (%)
CAT52					
275	28.5	13.8	0.2	1.6	12.9
315	39.9	25.2	0.9	3.7	10.1
350	50.4	18.8	4.2	13.2	14.2
375	52.6	16.6	12.1	20.2	3.7
275	13.5	3.5	0.4	1.9	7.7
CAT58					
275	67.8	49.2	0.2	7.2	11.2
315	66.1	39.4	2.0	13.5	11.2
350	57.4	13.6	10.4	21.8	11.6
375	63.8	5.2	21.0	18.0	19.6
275	31.8	19.9	0.7	2.8	8.4

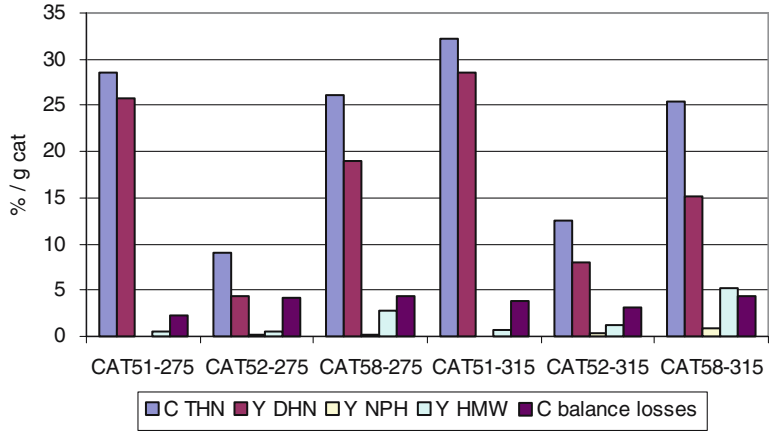

Figure 8. Conversion, yield and C-loss value (normalized for weight unit) determined for the three catalysts investigated (Temperature = 275 and 315 °C; contact time = 3.6 s; LHSV = 4 h^{-1}; H_2/THN molar ratio = 15.0).

–SiO_2 > Pd/Pt–TiO_2–WO_3, as well as the catalyst stability with the reaction temperature. The Pd/Pt–TiO_2 catalyst showed good performances in all the reaction conditions investigated, together with a good thio-tolerance up to at least 50 wt ppm of S.

Acknowledgments

The financial support by EU Commission's GROWTH Program (Contract No. G5RD-CT-2001-0537), MIUR (Italy) and CICYT (Spain, MAT03-2986) is gratefully acknowledged. Thanks are due to Millenium Chemicals for supplying the commercial supports.

References

[1] B.H. Cooper and A. Stanislaus, Catal. Rev. Sci. Eng. 36 (1994) 75.
[2] B.H. Cooper and B.B.L. Donnis, Appl. Catal. A137 (1996) 203.
[3] G. Murali Dhar, B.N. Srinivas, M.S. Rana, Manoj Kumar and S.K. Maity, Catal. Today 86 (2003) 45.
[4] S. Dzwigaj, C. Louis, M. Breysse, M. Cattenot, V. Belliére, C. Geantet, M. Vrinat, P. Blanchard, E. Payen, S. Inoue, H. Kudo and Y. Yoshimura, Appl. Catal. B41 (2003) 181.
[5] K. Ito, T. Tomino, M. Oshima, H. Kurokawa, K. Sugiyama and H. Miura, Appl. Catal. A249 (2003) 19.
[6] E. Lecrenay, K. Sakanishi, T. Nagamatsu, I. Mochida and T. Suzuka, Appl. Catal. B18 (1998) 325.
[7] Y. Ji, P. Afanasiev, M. Vrinat, W. Li and C. Li, Appl. Catal. A257 (2004) 157.
[8] Y. Saih and K. Segawa, Catal. Today 86 (2003) 61.
[9] M.S. Rana, S.K. Maity, J. Ancheyta, G. Murali Dhar and T.S.R. Prasada Rao, Appl. Catal. A253 (2003) 165.
[10] E.Y. Kaneko, S.H. Pulcinelli, V. Teixera da Silva and C.V. Santilli, Appl. Catal. A235 (2002) 71.
[11] S.K. Maity, J. Ancheyta, L. Soberanis, F. Alonso and M.E. Llanos, Appl. Catal. A244 (2003) 141.
[12] M. Jacquin, D.J. Jones, J. Rozière, S. Albertazzi, A. Vaccari, M. Lenarda, L. Storaro and R. Ganzerla, Appl. Catal. A251 (2003) 131.
[13] T. Fujikawa, K. Idei, T. Ebihara, H. Mizuguchi and K. Usui, Appl. Catal. A192 (2000) 253.
[14] S. Albertazzi, R. Ganzerla, C. Gobbi, M. Lenarda, M. Mandreoli, E. Salatelli, P. Savini, L. Storaro and A. Vaccari, J. Mol. Catal. A: Chem. 200 (2003) 261.
[15] M. Jacquin, D.J. Jones, J. Rozière, A. Jiménez López, E. Rodríguez-Castellón, J.M. Trejo Menayo, M. Lenarda, L. Storaro, A. Vaccari and S. Albertazzi, J. Catal. 228 (2004) 447.
[16] H. Yasuda and Y. Yoshimura, Catal. Lett. 46 (1997) 43.
[17] Shell Report No. 199.
[18] S. Albertazzi, E. Rodríguez-Castellón, M. Livi, A. Jiménez-López and A. Vaccari, J. Catal. 228 (2004) 218.
[19] R.F. de Farias, U. Arnold, L. Martinéz, U. Schuchardt, M.J. D.M. Jannini and C. Airoldi, J. Phys. Chem. Solids 64 (2003) 2385.
[20] Y. Wang, Q. Chen, W. Yang, Z. Xie, W. Xu and D. Huang, Appl. Catal. A250 (2003) 25.
[21] E. Pabón, J. Retuert, R. Quijada and A. Zarate, Microp. Mesop. Mater. 67 (2004) 195.
[22] S. Brunauer, L.S. Deming, W.S. Deming and E. Teller, J. Amer. Chem. Soc. 62 (1940) 1723.
[23] IUPAC Reporting Physisorption Data for Gas/Solid Systems, Pure Appl. Chem. 57 (1985) 603.
[24] A.D. Schmizt, G. Bowers and C. Song, Catal. Today 31 (1996) 45.
[25] B. Pawelec, R. Mariscal, R.M. Navarro, S. van Bokhorst, S. Rojas and J.L.G. Fierro, Appl. Catal. A225 (2002) 223.
[26] V.L. Barrio, P.L. Arias, J.F. Cambra, M.B. Güemez, B. Pawelec and J.L.G. Fierro, Catal. Commun. 5 (2004) 173.
[27] A. Spamer, T.I. Dube, D.J. Moodley, C. van Schalkwyk and J.M. Botha, Appl. Catal. A255 (2003) 153.
[28] L. Lietti, J.L. Alemany, P. Forzatti, G. Busca, G. Ramis, E. Giamello and F. Bregani, Catal. Today 29 (1996) 143.
[29] M.L. Occelli, S. Biz and A. Aurox, Appl. Catal. A183 (1999) 231.
[30] S. Klein, S. Thorimbert and W.F. Maier, J. Catal. 163 (1996) 476.
[31] S. Albertazzi, I. Baraldini, G. Busca, E. Finocchio, M. Learda, L. Storaro, A. Talon and A. Vaccari, Appl. Clay Sci. 29 (2005) 224.
[32] M. Skotak, D. Lomot and Z. Karpinski, Appl. Catal. A229 (2002) 103.
[33] M.A. Vicente and J.-F. Lambert, Phys. Chem. Chem. Phys. 3 (2001) 4843.
[34] S. Albertazzi, G. Busca, E. Finocchio, R. Glöckler and A. Vaccari, J. Catal. 223 (2004) 372.